AN EFFICIENT METHOD FOR MEASURING TRAPPED GAS SATURATION UNDER CO-CURRENT CONDITIONS

N. Bona, L. Garofoli, F. Radaelli, C. Zanaboni, M. Anelli, A. Bendotti and D. Mezzapesa
ENI e&p

This paper was prepared for presentation at the International Symposium of the Society of Core Analysts held in Avignon, France, 8-11 September, 2014

ABSTRACT

The amount of gas trapped by water influx is a critical parameter for the evaluation of the recoverable reserves of a large gas reservoir in Mozambique. We compare trapped gas saturation measurement results obtained by using various methods. All the tests were performed on the same six core samples. They differed from one another in the liquid used, the boundary conditions and the gravity force applied to the samples. The tests included: 1) spontaneous imbibition measurements on unsealed cores totally immersed in either toluene or water, 2) spontaneous imbibition measurements on laterally sealed cores with one end in contact with water and the other end exposed to air, 3) forced imbibition measurements by centrifuging unsealed cores under water with 1D NMR saturation profiling run in combination. The latter method is very efficient because it produces an exhaustive compilation of initial gas saturation vs. trapped gas saturation data.

The lab data are compared to the log data acquired in an interval below the gas-water contact, where current gas saturations are the result of the rise of a paleo-gas-water contact. We take these saturations as the reference. Tests 1) and 2) provided slightly high trapped saturations, probably due to the presence of countercurrent flow (mainly in test 1) and evaporation effects (only in test 2). For the centrifuge/NMR experiments a good match to the log data is obtained for Bond numbers in the $4\times10^{-6} – 5\times10^{-5}$ range.

INTRODUCTION

Spontaneous imbibition has been an active subject of research for decades. The first studies on spontaneous imbibition date back to the 1960s, but interest in this research area exploded in the 1990s, when fractured oil reservoirs became an important resource for hydrocarbon production. An exhaustive review of the theoretical and experimental work on spontaneous imbibition of water against oil done over the last 50 years can be found in Mason and Morrow (2013). The imbibition of water against gas is less well documented. In liquid-gas imbibition, rock wettability is not a variable and a strongly wetting preference to the liquid phase may be assumed. Nevertheless, the process is more complex than liquid-liquid imbibition because the non-wetting phase is compressible and can dissolve in the wetting phase. In a gas reservoir, water imbibition is caused by a gradual reduction of the pressure of the gas while this is produced from upper layers. The fraction of gas left behind the encroaching water front is referred to as the trapped gas saturation and is what we want to determine. The standard method for measuring trapped

gas saturation in the lab is based on multiple sequences of controlled evaporation and spontaneous imbibition measurements. A core sample is saturated with a liquid, then part of the liquid is allowed to evaporate in order to achieve a predetermined initial air saturation (Sgi). Once the desired Sgi value has been obtained, the core is brought into contact with the liquid allowing liquid imbibition. When no more liquid enters the core, the remaining air saturation (Sgr) is recorded. This is a function of Sgi. Because the initial gas saturation of a reservoir varies with depth from zero to a given irreducible value, in the lab several evaporation/imbibition cycles are usually performed, so that a number of Sgi-Sgr couples can be acquired and a more comprehensive picture of the behavior of the reservoir can be obtained. Typically, each sample undergoes four evaporation/imbibition cycles and the respective Sgi values are set at 100%, 75%, 50% and 25%. The amount of imbibed liquid is monitored versus time by weighing the core.

CURRENT TRAPPED GAS METHODS AND THEIR LIMITATIONS

The most common setup for a trapped gas experiment was first described by Pickell et al (1966). Some labs call it the Counter-Current Imbibition test (CCI). In a CCI experiment the core is unsealed, that is all the faces are open to flow (following Mason and Morrow, 2013, this boundary condition will be called AFO – all-faces-open). During imbibition the core is totally immersed in the liquid, typically toluene (Fig.1a). The majority of labs prefer an organic solvent over water because the evaporation stage to achieve initial air saturation is faster and there are no issues related to salinity variations. The boundary conditions of a CCI experiment generate a combination of linear and radial flows, and the flow is predominantly countercurrent (Baldwin and Spinler, 1999). Even if the gas flow is linearized by sealing the curved surface of the core (Fig.1b), the flow will remain essentially countercurrent if the core stays totally immersed in the liquid (Wickramathilaka et al., 2011). After Mason and Morrow (2013) we will call this boundary condition TEO (two-end-open). An improved methodology is to use a laterally coated core and keep it partially immersed in the liquid (Fig.1c). With this setup, the liquid will penetrate from the bottom face and imbibition is supposed to occur as capillary rise. This offers a higher chance of generating a co-current displacement, especially when the rock permeability is low. However, with permeabilities of hundreds of millidarcies or more, part of the gas will invariably be produced countercurrently from the bottom face of the sample (see picture 1c). Moreover, the liquid can evaporate from the top face of the sample during imbibition. It is quite difficult to mimic the process by which the gas becomes trapped by an encroaching aquifer. The reservoir process has three features: 1) gas displacement by water is co-current; 2) gas diffusion into the water is negligible; 3) during reservoir life, the rock is flowed by many pore volumes of water. The spontaneous imbibition experiments described above do not have all of these features: actually, the core is invaded by less than one pore volume of liquid and none of the examined boundary conditions can guarantee that the flow is totally co-current. Co-current flow conditions can be obtained only if a directional, driving force opposing capillarity is applied to the core. In this paper we investigate the use of the artificial gravity force generated by the centrifuge.

DESCRIPTION OF THE CENTRIFUGE/NMR METHOD (CNMR)

The CNMR method combines centrifuge measurements with saturation monitoring by 1D NMR. The starting point is to centrifuge a fully water saturated sample under air. The rotation generates an *x*-dependent initial gas saturation (Sgi) profile in the sample (Fig. 2). It is possible to keep the bottom end of the sample in contact with water. The rotational speed is set so that at the other end a low gas saturation value is achieved. Ideally, this should be of the same order of magnitude as the saturation existing in the reservoir far from the water-gas contact so as to cover a representative range of initial saturations. Then we perform a classic forced imbibition test. The sample is centrifuged under water at increasing speeds. At the end of each centrifugation we measure the remaining gas saturation (Sgr) profile in the sample. At each position along the sample length, Sgr is a function of the applied Bond number (N_b) and the Sgi value obtained after centrifuging in air. Typically we perform five rotational steps. With 40 positions, a compilation of 200 Sgi-Sgr- N_b triplets is produced. The Bond number is calculated from the formula $N_b = \Delta\rho g k/\sigma$, where $g = \omega^2 R$, $\omega = 2\pi f$, f = number of rotations per second, R = distance from the axis of rotation in metres, $\Delta\rho$ = water-air density difference in kg/m^3, σ = water-air interfacial tension in N/m, and k = sample permeability in m^2 (it is assumed that permeability is constant throughout the sample). In order to obtain representative Sgi-Sgr data points, it is mandatory to have representative N_b values. We will see later how they are obtained.

It is assumed that water imbibition is a mono-dimensional process, that is Sg varies only along the sample length, not in transverse directions. Each time that the centrifuge is stopped, the fluids in the sample tend to redistribute. We monitored the return of Sg to equilibrium on a couple of sister samples and observed that despite the high permeability of the rock it took several days before the Sg distribution changed significantly. Because the time that elapses between two consecutive centrifugations is of order of tens of minutes, saturation redistribution should not have affected the measurements presented in this paper.

MATERIAL AND EXPERIMENTS

The core samples investigated in this study were taken from a gas field in Mozambique that hosts over 80 TCF of natural gas in place. The field is comprised of several reservoirs. The reservoir under analysis is formed by turbidite channel and lobe deposits of several deepwater basin floor fan accumulations and consists of coarse and massive sandstones that are extraordinarily thick, clean and homogeneous. Porosity is around 20% and permeability is around 1 darcy. We performed the following experiments:

a) **AFO_{tol}** = Classic toluene-air spontaneous imbibition experiments on samples immersed in toluene with all faces open to flow (Fig.1a). Four initial gas saturations (Sgi = 25%, 50%, 75% and 100%) were tested.
b) **AFO_w** = the same as a) but with brine and on initially dry samples (Sgi = 100%).
c) **TEO** = Water-air spontaneous imbibition measurements on coated samples, with one end in contact with brine and the other end exposed to air (Fig.1c). These experiments were performed on initially dry samples (Sgi = 100%).

d) **CNMR** = Forced water-air imbibition experiments by using the centrifuge/NMR method. A range of initial gas saturations was tested.

The same six samples were used in all these experiments. All the experiments were carried out at ambient conditions. In experiments AFO_{tol}, AFO_w and TEO, air recovery was monitored versus time by weighing the sample during imbibition. This permitted us to investigate air solubility effects in terms of both intensity and timing. In the CNMR test we measured only the final air saturations.

GAS SOLUBILITY EFFECT AND ITS CORRECTION

While gas diffusion into water is probably negligible in the reservoir, liquid-gas imbibition experiments are affected by gas solubility effects. The standard procedure to correct for such effects relies upon the assumption that spontaneous imbibition is an essentially immiscible displacement (capillary-dominated regime) till a certain instant and then becomes essentially miscible (diffusion-dominated regime). The crossover between the two regimes is determined by plotting the gas saturation of the sample vs. the square root of time. In theory two linear trends should be seen. The gas saturation of the sample at the crossover time is conventionally named SgrM and is supposed to give a representative estimate of trapped gas saturation. SgrM represents the main output of a classic trapped gas saturation measurement (Hamon et al, 2001). In the experiments reported in this paper, the slope of the straight line associated with diffusion was found to range from -2×10^{-1} to -4×10^{-3} %PV/$\sqrt{s}$ with an average of -7×10^{-2} %PV/$\sqrt{s}$. This means that after 10, 100 and 1000 seconds of imbibition the average loss of gas saturation due to diffusion was of 0.2, 0.7 and 2.4 saturation units, respectively. No significant differences were seen when passing from water to toluene or changing the initial air saturation of the samples. In the AFO_{tol}, AFO_w and TEO experiments, we determined SgrM directly from the respective Sg vs $\sqrt{time}$ curves. In the CNMR experiments, we calculated the gas lost by diffusion in each centrifugation step from $Sg_{lost} = 7\times10^{-2}\sqrt{centrif\ time}$ [%PV]. Then we added this quantity to the gas saturation measured by weighing the sample to obtain a corresponding SgrM value. The centrifugation times were all of the order of 1200 s.

RESULTS – PART 1: SPONTANEOUS IMBIBITION

Tab.1 summarizes the results of the spontaneous imbibition experiments AFO_{tol}, AFO_w and TEO: tc is the duration of the capillary regime, i.e. the amount of time that elapsed between the first contact of the sample with the liquid and the end of the capillary-dominated regime; tt, is the duration of the test, i.e. the amount of time during which the sample remained in contact with the liquid; SgrM is the trapped air saturation value obtained as described in the previous section; and SgrF is the final air saturation of the sample calculated from the sample weight at the end of the test. While the slopes of the straight lines associated with the diffusion regime did not vary significantly with either the liquid type or the initial saturation of samples, SgrM and the duration of the capillary-dominated regime appeared to be strongly dependent on both the liquid type and Sgi.

Effect of liquid type. The dependence of SgrM on liquid type can be appreciated by comparing AFO_{tol} at Sgi =100% with AFO_w (these experiments were conducted with the same boundary condition and initial saturation). The trapped gas saturation SrgM appears to be systematically lower in AFO_{tol}. On average, a difference of 4.0 saturation units is observed. Also the duration of the capillary regime appears to be dependent on the liquid used. For the tests conducted with toluene this was found of the order of 80 seconds, whereas those performed with water exhibited durations of 290 seconds on average. Only one sample (# 61) showed similar tc values in the AFO_{tol} and AFO_w experiments. It may be interesting to note that these results are not in full agreement with the scaling relationships proposed by Wang R (1997) and Zhou et al. (2002) after Ma et al. (1997). Following Wang, the recovery time of gas by water (t_w) divided by the recovery time by toluene (t_{tol}) should equal quantity $\frac{\sigma_{tol}}{\sigma_w}\left(\frac{\mu_w}{\mu_{tol}}\right)^{0.8}$. With μ_w= 1.0 cp, σ_w= 72 dynes/cm, μ_{tol}= 0.59 cp and σ_{tol}= 28 dynes/cm, a t_w/t_{tol} ratio of 0.6 is obtained, whereas our experiments gave a water/toluene tc ratio of 3.8, on average (we consider the gas recovery time and the duration of the capillary regime as synonymous). The equation of Zhou et al., which incorporates the mobility ratio, gives $t_w/t_{tol} \approx \frac{\sigma_{tol}}{\sigma_w}\sqrt{\frac{\mu_w}{\mu_{tol}}\frac{k_{rtol}}{k_{rw}}}$, where k_{rtol} and k_{rw} are characteristic values of the relative permeability to the two liquids (with gas as the other phase). Substituting the experimental value t_w/t_{tol}=3.8 and solving for $\frac{k_{rtol}}{k_{rw}}$ gives a value of 0.02, which is too low.

Effect of initial saturation. The dependence of SrgM and the duration of the capillary regime on initial gas saturation is illustrated in Fig.3 and Fig.4 for AFO_{tol}. Fig.3 confirms the well known fact that trapped gas saturation increases with initial gas saturation up to a maximum value and then tends to exhibit a plateau. Fig.4 shows that also the duration of the capillary-dominated regime increases as Sgi increases. The higher the initial amount of liquid in the sample, the faster the imbibition process. This fact can be explained by considering that with a higher initial liquid saturation the chance of having snap-off mechanisms ahead of the liquid front is greater. These add to the piston-like air displacement processes that take place behind the front, thus increasing the overall amount of displaced gas.

Effect of boundary conditions. The effect of boundary conditions on both trapped air saturation and duration of the capillary-dominated regime can be investigated by comparing the results of the AFO_w and TEO experiments, which were conducted with brine on initially dry samples. As can be seen in Fig.5, AFO_w gave shorter imbibition times and lower SgrM values. In the plot, the empty and solid triangles represent two separate series of TEO experiments. One was performed by setting the free water level around the sample a few millimeters above its bottom face; in the other the FWL was placed a few millimeters above the sample top (a long heat-shrink tube prevented the water from contacting the top end). The fact that SgrM from AFO_w is lower than from TEO was unexpected: with a countercurrent flow there is a higher chance of isolating the

non-wetting phase and the proportion of countercurrent flow in AFO_w should be greater than in TEO. Probably, TEO gave high SgrM values because of the evaporation of a certain amount of water from the top face of the samples during imbibition. Part of the flow was certainly countercurrent also in TEO. As a matter of fact, several air bubbles were seen to emerge and grow from the bottom face of the samples at the onset of imbibition (Picture 1c). These bubbles stayed attached to the sample all the time, progressively reducing the surface area open to imbibition. Perhaps that can explain why the capillary regime lasted longer in TEO.

RESULTS – PART 2: FORCED IMBIBITION

The results of the forced imbibition measurements carried out with the CNMR method are illustrated in Fig.6. Each data point is associated with a given position along the sample and a given centrifugation step. The *x*-coordinate represents the initial air saturation (Sgi) in that position, while the *y*-coordinate is the remaining air saturation (Sgr) after that centrifugation step. Sgr does not depend only on Sgi, but also on the Bond number $N_b = \Delta\rho gk/\sigma$, which, in turn, is a function of the position and the rotational speed. All Sgr values have been corrected for diffusion, as previously described.

Critical Bond number for trapped gas mobilization. Plotting Sgr versus the respective Bond number, for any given position, we obtain curves such as that illustrated in Fig.7. Sgr appears to decrease gradually as the applied Bond number increases. As the Bond number exceeds a certain critical value, Sgr decreases at a much faster rate. It is not difficult to define the critical value, which appears to be in line with published results for the mobilization of trapped blobs of non-wetting residual phase. The critical Bond number values determined by analyzing the available Sgr vs. N_b curves are of the same order of magnitude as quantity $0.02 \cdot kr^{-2}$, where k is the permeability in m^2 and r is the average pore threshold radius in metres. Actually, this expression is known to represent a measure of the critical Bond number (Oughanem et al., 2013). Consider a trapped air cluster: the gravity force acting on the cluster is proportional to the differential pressure across it, i.e. to quantity $\Delta\rho gl$, where l is the size of the cluster. The capillary force resisting cluster mobilization is proportional to $2\sigma/r$, where σ is the water-air interfacial tension and r is the mean pore threshold radius. The capillary force prevails over the gravity force if $\Delta\rho glr/(2\sigma) < 1$. Multiplying both members by $k/(rl)$ gives $\Delta\rho gk/\sigma < 2k/(rl)$, that is $N_b < 2k/(rl)$. The rock under test has a mean pore threshold size r of the order of 3×10^{-5} m (see the MICP curve in Fig.8) and a permeability of the order of 1×10^{-12} m^2. For the cluster size we hypothesize a maximum value l of the order of $50\times r$ (published results show that most of the volume occupied by the residual non-wetting phase is taken by clusters spanning over various pore distances - see Khishvand et al. (2013), Youssef et al. (2013), Raeesi and Morrow (2013) and references therein). Substituting gives $N_b < 5\times10^{-5}$, which is consistent with the experimental SgrM vs. N_b curves.

Critical Bond number for co/counter-current transition. The Sgr values obtained with the CNMR method are considered to be valid and representative only if the Bond number associated with them is less than 5×10^{-5}. However, besides this critical value, we must define also a critical Bond value setting the crossover from countercurrent to co-current flow. In the AFO_{tol}, AFO_w and TEO experiments, the g value applied to the samples (g = 9.8 m/s^2) honors the condition for residual air mobilization but not that for co-current flow. We expect a relationship between Sgr and the applied Bond number such as that schematically shown in Fig.9. While the literature has plenty of studies on the critical Bond number for residual phase mobilization, little data have been published on the critical value for the counter/co-current flow transition. Studying low IFT imbibition, Schechter et al. (1994) make use of an inverse Bond number defined as $Bo^{-1} = 0.4\cdot\sigma\sqrt{\phi/k}/(\Delta\rho gH)$ (metric units) and conclude that if $Bo^{-1} > 5$ the imbibition is driven by capillary forces (countercurrent flow), whereas if $Bo^{-1} < 1$ the imbibition is dominated by gravity forces (vertical co-current flow). For intermediate values of Bo^{-1} a combination of the two imbibition mechanisms is expected. Here H is the length of the core sample and ϕ the porosity. The ranges proposed by Schechter et al. are consistent with the simulations performed by Hosein Kalaei et al. (2010). The $Bo^{-1} < 1$ condition can be rearranged to obtain $\Delta\rho gk/\sigma > 0.4\sqrt{k\phi}/H$, that is $N_b > 0.4\sqrt{k\phi}/H$. There is an interesting physical meaning in this relation. It can be written as $N_b > 2k/(rH)$, with $r = 5\sqrt{k/\phi}$. Although the latter relationship is strictly valid for a cubic network of capillary tubes (Dullien, 1979), it has been used also to model real rocks. As discussed in the previous section, inequality $N_b > 2k/(rH)$ represents the condition required for the mobilization of a gas cluster of size H. At the onset of imbibition, the core contains a continuous gas phase and from a geometrical point of view this corresponds exactly to a cluster of size H. If the applied Bond number is such that $N_b > 2k/(rH)$, then this gas will be mobilized upward, and this is equivalent to saying that the flow will be co-current. With $k = 1\times10^{-12}$ m^2, ϕ = 0.2 and H= 0.05 m, the Schechter et al. condition for co-current flow gives $N_b > 4\times10^{-6}$.

Valid CNMR results. By combining the two conditions found for N_b, we argue that the valid data points in Fig.6 are those with N_b in the $4\times10^{-6} - 5\times10^{-5}$ interval. Fig.10 highlights these values. In the plateau region, Sgr ranges from 20% to 25% with an average value around 23%. We do not have a conclusive explanation for the scatter in the Sgr values when Sgi is around 20%. These data points come all from the two samples with the lowest permeability values (#27 and #68) but do not appear to be correlated with either the Bond number or the position along the core length. A final remark on the centrifuge/NMR method: before starting the centrifuge, the sample stays immersed in water with all faces open for a few minutes, i.e. the amount of time needed to balance the core holders. Countercurrent imbibition takes place during this time, but its effects are assumed to be cancelled by the forthcoming forced imbibition.

Air compressibility effects. Every time the centrifuge is stopped, the air pressure falls and the air in the core expands. As a result, the air saturation derived from sample

weight may be higher than that existing while centrifuging. The air expansion results in a saturation increase if part of the water is expelled from the core. This may be the case for trapped air clusters, whereas the air that is connected to the outside of the core should drain little amounts of water with consequent little impacts on air saturation. Depending on the rotational speed and the distance from the axis of rotation, we calculate that in the CNMR experiments the absolute pressure of air ranged from approx. 1.1 bar to approx. 6.0 bar while centrifuging and when the centrifuge was stopped the air volume increased by a factor ranging from 1.003 to 5.60. The 1.003 factor is for air at the core outlet (close to the axis of rotation) after centrifuging at the lowest rotational speed. The 5.60 factor applies to the core inlet and the highest speed. Correcting the valid ambient Sgr values illustrated in Fig.10 for air compressibility gives the "while centrifuging" values shown in Fig. 11. These were obtained by assuming that all the air expansion resulted in a corresponding water expulsion, so they should represent the minimum possible values of Sgr. As can be seen, the scatter in the plateau region increases and the average Sgr decreases by a few saturation units. It is really complex to determine how much water was actually expelled during gas expansion. We tend to think that because the trapped saturations obtained from the spontaneous imbibition experiments are not dramatically different from the CNMR saturations and the latter appear to be in line with the log data (see next section), air compressibility effects did not play a role of primary importance. In partial support of this assumption, the residual air saturation values obtained from the production profiles registered during water-air injection tests conducted on sister samples are not very different from the residual saturations estimated by weighing at ambient pressure after dismounting the samples from the core holders. In theory, air compressibility has an impact also on the definition of the valid Bond number range, given that N_b depends on the water-air density difference and the critical value for the mobilization of trapped blobs is a function of the length of the air blobs. Both quantities increase when the centrifuge is stopped, but that does not affect the CNMR result to a significant extent.

Log data. The log interpretation is shown in Fig.12. The gas-water contact is located at XX38 m (by gas-water contact it is meant the lowest point at which gas is considered to be mobile). Between XX38 and XX62 m there is the transition zone. The thickness of the transition zone is consistent with the capillary characteristics of the rock, as determined from conventional capillary pressure and MICP analyses. A shale layer is observed between XX62 and XX84 m. A thick zone containing immobile gas is seen beneath the shale. This gas results from the rise of a paleo-water contact. Because the petrophysical characteristics of the rock do not seem to vary above and below the shale layer, the observed immobile gas saturation is assumed to be representative of the trapped saturation that will form in the reservoir when production starts. The Sg values immediately below the shale layer are relatively high due to the accumulation of the gas. Below XX94 m, for a considerable thickness, Sg appears to range from 5% to 30% with an average value of 20%. This behavior is in line with the CNMR results. The Archie model was utilized for the interpretation of the electric logs (the clay content of the rock is very low). In absence of imbibition data, the saturation exponent derived from primary

drainage experiments was used throughout. That might have caused underestimated Sg values in the immobile gas zone where the imbibition n would have been more appropriate. However, due to the strongly water-wet conditions of the system, the impact is expected to stay within 5 saturation units. Adding this amount to the reported log-derived gas saturations would make the log data even closer to the CNMR results.

CONCLUSIONS

Spontaneous imbibition measurements of liquid against air involve both co-current and countercurrent flows. The high permeability samples examined in this study exhibited a non-zero fraction of countercurrent flow even when they were laterally sealed and the top end was exposed to air. The proportions of countercurrent and co-current flows depend on the applied Bond number. This is defined as $N_b = \Delta\rho g k/\sigma$. The flow is 100% co-current if $N_b > 0.4\sqrt{k\phi}/H$. In order to avoid mobilization of blobs of residual gas, the relation $N_b < 0.02 \cdot \mathrm{kr}^{-2}$ must also be satisfied. A trapped gas method combining centrifuge and NMR measurements is discussed. The method is very efficient because it gives many Sgi-Sgr data points per analyzed sample. The Sgr values obtained from this method are consistent with log measurements, whereas the values obtained from spontaneous imbibition experiments appear slightly higher.

REFERENCES

1. Baldwin B.A., Spinler E.A.:"In-situ saturation development during spontaneous imbibition", SCA-9922, 1992.
2. Dullien, F.A.L: "*Porous Media: Fluid transport and Pore Structure*", Academic Press, New York City, 1979.
3. Hamon G., Suzanne K., Billiotte, J., Trocme V.: "Field-wide variations of trapped gas saturation in heterogeneous sandstone reservoirs", SPE 71524, 2001.
4. Hosein Kalaei M., Green D.W., Willhite, G.P., "Numerical modeling of the water imbibition process in water-wet laboratory cores", SPE 132645, 2010.
5. Khishvand M., Akbarabadi M. Piri M., "Trapped non-wetting phase clusters: an experimental investigation of dynamic effects at the pore scale using a micro-CT scanner", SCA 2013-24, 2013.
6. Ma S., Morrow N.R., Zhand X.: "Generalized scaling of spontaneous imbibition data for strongly water-wet systems, *JPSE*, 18 (1997), 3/4, 165-178
7. Mason G, Morrow N.R., "Developments in spontaneous imbibition and possibilities for future work", *JPSE*, 110 (2013), 268-293
8. Oughanem R., Youssef S., Peysson Y, Bazin B., Maire E., Vizika O., "Pore-scale to core-scale study of capillary desaturation curves using multi-scale 3D imaging", SCA 2013-27, 2013.
9. Pickell J.J., Swanson B.F., Hickman W.B., "Application of air-mercury and oil-air capillary pressure data in the study of pore structure and fluid distribution", *old SPE Journal*, March 1966, 51-65.
10. Raeesi B., Morrow N.R., "Pore network modeling of experimental capillary pressure hysteresis relationships", SCA 2013-15, 2013.
11. Schechter D.S., Zhou D., Orr F.M., "Low IFT drainage and imbibition", *JPSE*, Vol. 11 (1994), 283-300.
12. Wang R.: "Gas recovery from porous media by spontaneous imbibition of liquid", MS thesis, University of Wyoming, 1999.
13. Wickramathilaka S., Howard J.J., Stevens J.C., Morrow N.R., Mason G. Haugen A., Graue A., Ferno M.A., "Magnetic resonance imaging of oil recovery during spontaneous imbibition from cores with two-ends open boundary condition", SCA 2011-24, 2011.
14. Youssef S., Deschamps H., Dautriat, J., Rosenberg E., Oughanem R., "4D imaging of fluid flow dynamics in natural porous media with ultra-fast X-ray microtomography", SCA 2013-12, 2013.
15. Zhou D., Jia L., Kamath J., Kovscek A.R.: "Scaling of counter-current processes in low-permeability porous media", *JPSE*, 33 (2002), 61-74.

				AFO - toluene/air				AFO - brine/air				TEO - brine/air			
sample #	Poro [%]	Perm [md]	Sgi [%]	tc [s]	tt [s]	SgrM [%]	SgrF [%]	tc [s]	tt [s]	SgrM [%]	SgrF [%]	tc [s]	tt [s]	SgrM [%]	SgrF [%]
14	20.2	1286	100	70	277	28.6	27.6	367	1793	23.1	20.7	1122	3290	32.7	30.1
			75.5	55	312	26.6	24.6								
			50.9	29	393	22.2	21.1								
			27.0	7	139	12.8	12.5								
27	19.4	851	100	98	304	25.8	25.4	469	2637	23.0	20.8	1789	10629	33.1	30.7
			75.9	51	287	25.6	23.9								
			51.9	28	196	21.2	20.6								
			27.7	11	186	14.8	14.8								
58	21.8	1370	100	63	196	26.9	26.5	319	8736	23.6	20.1	928	3522	34.9	32.9
			75.7	50	298	25.6	24.3								
			51.4	35	514	23.7	22.6								
			27.1	13	300	15.6	15.5								
61	21.3	1334	100	66	371	27.3	26.9	62	1894	25.7	25.7	1321	3101	37.3	35.7
			75.8	49	244	26.7	25.5								
			51.3	35	331	22.8	22.0								
			27.3	14	358	14.8	14.2								
64	20.3	1265	100	59	277	28.6	27.7	148	2256	21.0	20.9	1159	2516	33.5	32.3
			75.8	22	263	27.2	26.1								
			51.6	17	280	23.9	22.0								
			27.4	9	295	15.2	14.5								
68	21.6	792	100	89	315	27.3	26.5	379	2246	24.4	23.3	1969	7884	36.6	35.2
			75.5	62	307	27.2	26.5								
			51.6	38	283	22.9	22.5								
			27.0	12	215	15.3	15.1								

Tab.1: Results of spontaneous imbibition measurements

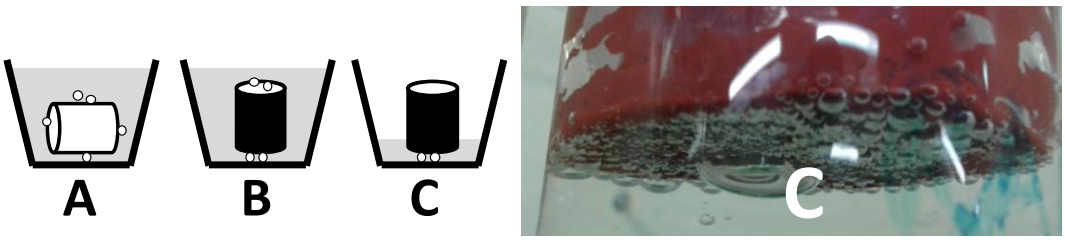

Fig.1: Boundary conditions for spontaneous imbibition experiments

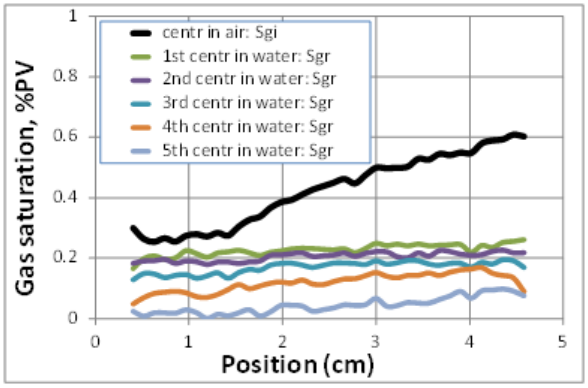

Fig.2: Gas saturation profiles measured on one of the analyzed samples

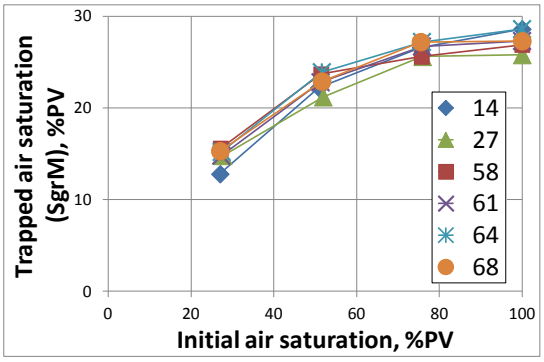

Fig.3 - AFO_{tol} experiments

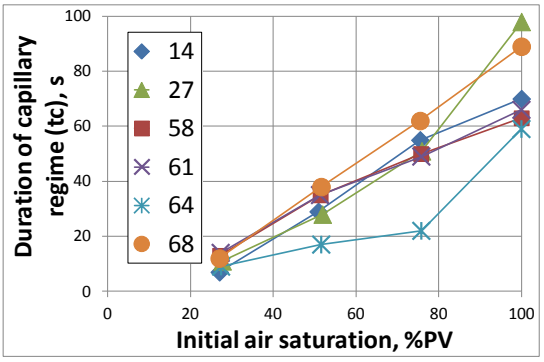

Fig.4 - AFO_{tol} experiments

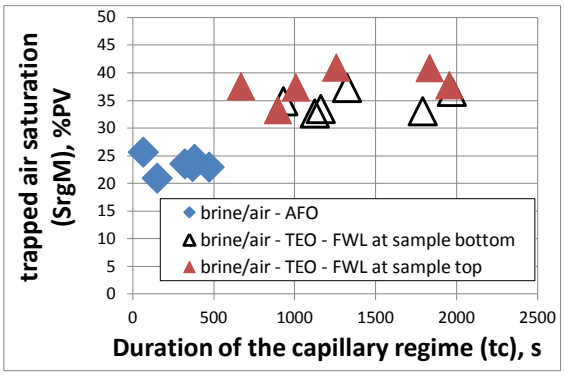

Fig.5 – Comparison of AFO_w and TEO results

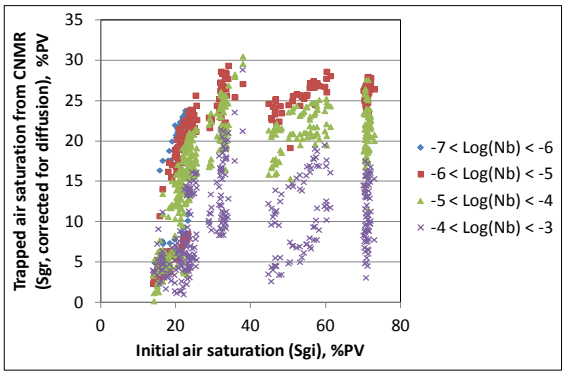

Fig.6 – CNMR results

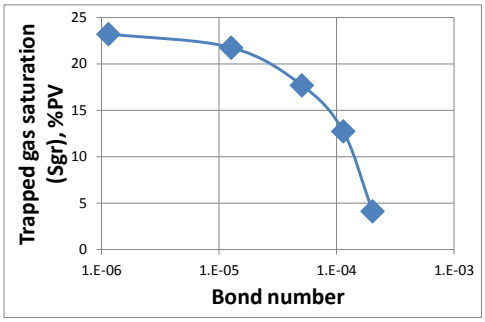

Fig.7 – Example of Sgr - Nb curve (sample 14, position: 2.25 cm)

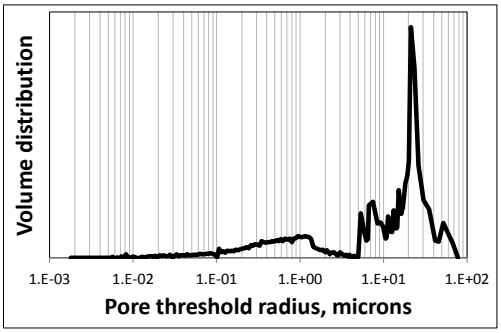

Fig.8 – Example of MICP curve (sample 27)

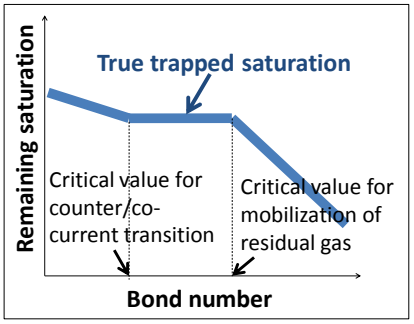

Fig.9 – Expected Sgr-Nb relationship

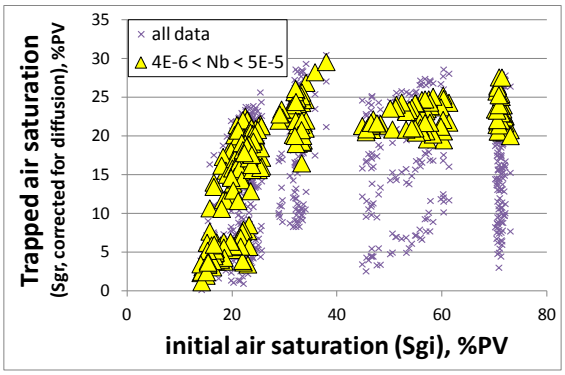

Fig.10 – Valid Sgi-Sgr data

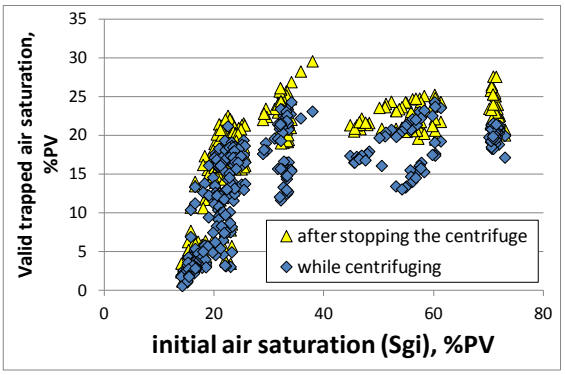

Fig.11 – Effect of air compressibility on CNMR results

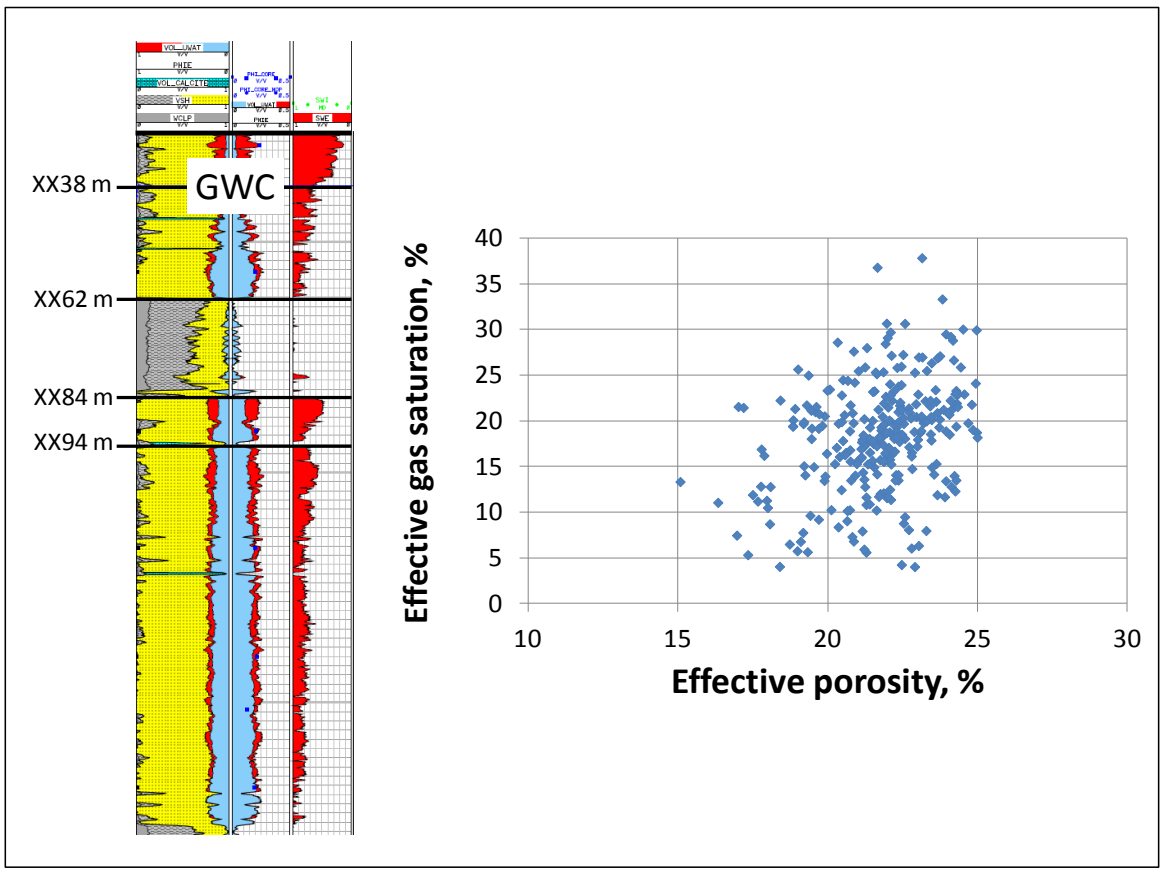

Fig.12 – Log data from below the water-gas contact